



Adsorption of eriochrome black T dye using alginate crosslinked *Prunus avium* leaf mediated nanoparticles: characterization, optimization and equilibrium studies

Tariqul Islam^{a,b}, Tong Ye^c, Changsheng Peng^{a,d,*}

^aThe Key Lab of Marine Environmental Science and Ecology, Ministry of Education, Ocean University of China, Qingdao 266100, China, email: tariq.bau@gmail.com (T. Islam)

^bDepartment of Agricultural Construction and Environmental Engineering, Sylhet Agricultural University, Sylhet-3100, Bangladesh

^cThe Key Lab of Marine Environmental Science and Ecology, Ministry of Education, Ocean University of China, Qingdao 266100, China, email: yetong1993@163.com (T. Ye)

^dSchool of Environment and Chemical Engineering, Zhaoqing University, Zhaoqing 526061, China, Tel. +86 532 66782011, Fax +86 532 66782011, email: pcs005@ouc.edu.cn, cspeng@ouc.edu.cn (C. Peng)

Received 10 January 2018; Accepted 10 August 2018

ABSTRACT

The adsorption capacity of alginate crosslinked *Prunus Avium* (*P. Avium*)/cherry leaf mediated nanoparticles (Alg-Ch-NPs) for anionic dye Eriochrome Black T (EBT) was studied in this article. The *P. Avium* leaf mediated nanoparticles (NPs) were made by capping the functional groups from the cherry leaf extract with Fe₂SO₄ and FeCl₂ solution in 1:2 ratio. Surface of the NPs was modified by adding the green NPs with prepared Ca alginate gel, especially to get more positive charges to adsorb anionic dyes. Characterizations of the adsorbent were conducted by using ultra violet spectroscopy (UVS), fourier transform infrared spectroscopy (FTIR), x-ray diffraction (XRD), scanning electron microscopy (SEM), energy dispersive x-ray spectroscopy (EDX) and transmission electron microscopy (TEM). The effects of various reaction conditions such as contact time, initial concentrations, dosages, pH and ionic strength on adsorption of EBT dye using Alg-Ch-NPs were studied. Langmuir, Freundlich and Tempkin isotherm models were used to analyze adsorption equilibrium isotherms, and it was found that the Freundlich isotherm model was best fitted with the experiment data. As well as, pseudo-first-order and pseudo-second-order kinetic models were used in kinetic experiments on the data, and it was found that pseudo-first-order kinetic model was most suitable. In addition, Weber's intraparticle diffusion model was also used to gain the adsorption mechanisms and furthermore boundary layer effect of the adsorbents was found. The maximum adsorption capacity of Alg-Ch-NPs on EBT dye was 85.66 mg/g, which is significantly higher compared with other studies on adsorption of EBT dye.

Keywords: Adsorption; Alginate crosslinked NPs; Plant mediated NPs; Anionic dyes; Green nanotechnology

1. Introduction

The use of NPs is rising rapidly for their easy using techniques and their efficiency removing organic and inorganic pollutants from wastewater [1]. At present, iron NPs

are used in the process of environmental remediation for their extensive and unique characteristics like higher surface area in comparison to corresponding bulk forms, small size (1 to 100 nm), tunable nature of different properties and higher reactivity [2,3]. The application of nanoscience in the biomedicine, food, cosmetic, electronic and environmental field for its exceptional characteristics [3,4]. Enor-

*Corresponding author.

mous uses of nanomaterials by scientific community have been released scientific research, publications, projects and patents [5]. Application of nanomaterials is to transform, degrade or destroy pollutants in different environment, such as water, air, soil etc. [6]. NPs have the capability to percolate through capillary pores of soil and suspend in water, and can disperse better and reach to location rapidly than the larger particles [7,8].

The green routes are used for NPs synthesis, avoiding the toxic by-product and making environmentally friendly manufacturing process [9]. Functionalizing NPs by using plant extracts is one of the low cost, simple and eco-friendly methods in green NPs production. In the NPs synthesis process plant extract played a dual role, one is to reduce the metallic salts and the other is to hinder the aggregation of NPs by acting as stabilizing agent. Plants extracts contain different compounds such as phenols, terpenoids, proteins and carbohydrates etc. [5]. The extracts from various plants contain different concentrations and combinations of reducing and stabilizing agents. Therefore, the compositions of extracts determine the characteristics and efficiency of NPs [10]. In this work a green route has been developed to produce iron NPs by cherry leaf extracts.

The physical and chemical properties are determined by the immobilization matrix. Adequate adsorption capacity depends on the selection of appropriate matrix [11]. Alginate, silica, polyvinyl alcohol and other different compounds were used as immobilization matrixes [11,12]. Immobilizing iron oxide NPs onto alginate could synthesize another hybrid material. The material has been made by combination of the excellent features of functionalized iron NPs cherry leaf extracts with alginate [3]. In this work, the capacity of the new material as adsorbent was studied for removal of Eriochrome Black T (EBT) dye, a toxic textile pollutant in wastewater as anionic species [13].

Dyes are colored matter originated from synthetic source which resist the exposure of light into water [14]. Dyes contain high organic compounds, non-biodegradable and complex aromatic structure [15]. Growth of aquatic plants and organisms can be hindered in presence of dyes by blocking the sunlight and reducing the re-oxygenation capacity [16]. In addition, presences of dyes in wastewater also have carcinogenic and mutagenic effects [17]. All over the world mostly azo dyes are used in textile industries. Azo dyes contains azo bonds (-N=N-), which act as chromophore in the molecular structure [18]. Consequently, due to high resistance of light, heat, chemical and microbial attack, it is considered complicated to degrade the azo dyes even at low concentrations [19]. Finally, it is very much important to remove azo dyes from industrial effluents before they are discharged into water bodies or environment. An unique material has been deployed by green synthesis of iron oxide nanoparticles encapsulate with alginate compounds. Different type of sorption studies including the pH dependence, initial concentrations dependence, ionic strength effects, isotherms and kinetics equilibrium studies have proved the efficiency of new synthesized nanomaterials on EBT dye adsorption. The purpose of this study is to synthesize a new functionalized nanoparticle by eco-friendly method, to characterize the newly synthesized material, and to apply the prepared materials for adsorption of anionic dyes from aqueous solutions.

2. Materials and methods

2.1. Preparation of adsorbent

The *P. avium* leaves generally called as cherry leaves were collected from the Cherry Avenue, Ocean University of China (OUC). Then the collected samples were washed thoroughly with distilled water to remove the dust and foreign materials on the surface of the leaves. The samples were dried for 24 h at room temperature and again dried in oven at 100°C for 4 h to remove the total moisture in the leaves [20]. The dried samples were manually grinded in lab. The sample powder were sieved through a 1 mm sized sieve and stored in a sterile zip lock bag for further use. Then 20 g of prepared powders were added into 200 mL distilled water to make plant extracts. The prepared solution was vigorously stirred (150 rpm) in magnetic stirring machine (DRAGON LAB, MS7-H550-Pro) at 80°C for 3h. Then the solution was filtered by vacuum filter to separate the extract. The filtration was conducted with the filter of 0.45 µm pore size (Sartorius AG, 37070 Goettingen, Germany). Further, the iron solution made by Fe₂SO₄ and FeCl₂ with 1:2 ratio was added to the cherry leaf extract under vigorous stirring (150 rpm at 60°C temperature), the color of the solution changed from dark green to black [20]. The appearance of the solution changed into black indicating the formation of nanoparticles. This phenomenon was due to the reduction of iron salt in solution after adding plant extracts. Subsequently, an alginate gel was prepared by adding Na alginate (NaC₆H₇O₆) solution in 6% CaCl₂ solution [13]. The model structure of the formed gel is shown in Fig. 1. The black iron oxide solution was added slowly into the formed Ca-alginate gel under 150 rpm stirring at 30°C temperature. After the formation of opalescent suspension the prepared solution was centrifuged at 1000 rpm speed by an electric centrifuge machine (ROVSUN Desktop Electric Centrifuge Machine) for 30 min. The obtained solution was filtered with the filter of 0.45 µm pore size (Sartorius AG, 37070 Goettingen, Germany), dried in oven (JSOF-150) at 100°C to remove the moisture in it, and then stored in room temperature within sterile zip locked bag for further studies.

2.2. Preparation of eriochrome black T (EBT) solution

The EBT dye (produced by Nanjing Chemical Reagent Co. Ltd.) was collected from "Taobao", an online market in China. It was used without further purification and the chemical composition was analytical grade. The molecular structure of EBT is shown in Fig. 2 and the properties of EBT dye are listed in Table 1 [21]. The 1000 mg/L concentrations' solution of EBT dye was prepared by diluting chemical dye with distilled water for further use.

2.3. Determination of pH of point of zero charge (pH_{pzc}) of the adsorbent

In order to determine the pH of point of zero charge (pH_{pzc}), 0.5 gm of Alg-Ch-NPs was taken in 5 different 300 ml conical flasks containing 100 ml of 0.01 M NaCl. The pHs of the solutions contained by different flasks was adjusted to 2, 4, 6, 8 and 10 by adding 0.01 M HCl or NaOH. After

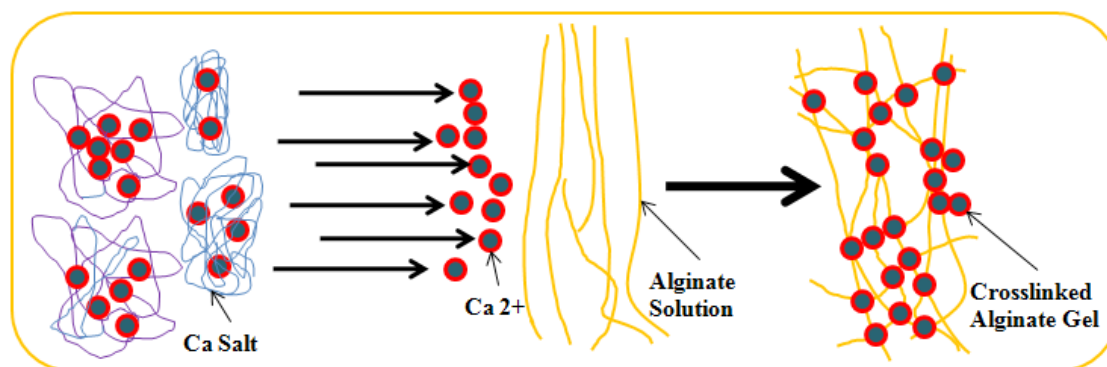


Fig. 1. Formation procedure of Ca alginate gel.

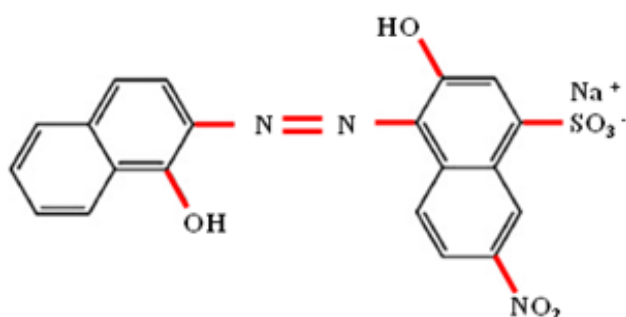


Fig. 2. Molecular structure of EBT dye.

Table 1
Characteristics of EBT dye

Type of dye	Anionic azo dye
Chemical formula	$C_{20}H_{12}N_3O_7SNa$
Molar mass	461.38 g/mol
Maximum wavelength	530 nm
Solubility in water	50 g/L
Solubility in ethanol	2 g/L
Appearance	Black

labeling, the prepared flasks were sealed and placed in a shaker with 150 rpm shaking at 30°C temperature for 24 h. The solutions of the flasks were filtered with a vacuum filter and the pHs were measured by pH meter [22].

2.4. Batch adsorption studies

Adsorption experiments were completed at 30°C temperature and 150 rpm in a mechanical shaker. The experiment was carried out on several flasks containing different known concentrations of dyes such as 10 mg/L, 50 mg/L, 100 mg/L, 150 mg/L and 200 mg/L with required dosages of adsorbents for the specific time period (10–200 min). The initial pHs of the solutions were measured to know the optimum pHs. The pHs of the solutions were changed by adding 1 M HCl or 1 M NaOH solution. At the equilibrium time

of the solutions, the final concentrations (c_e) were measured by taking absorbance from spectrophotometer and comparing with the absorbance value of the initial concentrations of the solutions (C_0) [23]. The maximum wavelength for the EBT dye was considered to be 530 nm in the measurement of absorbance for different concentrations of dyes. The removal percentages of EBT dye was calculated by the following equations [23];

$$\% \text{ Dye Removal} = \frac{C_0 - C_e}{C_0} \times 100 \quad (1)$$

where c_0 denotes initial concentrations and c_e denotes equilibrium concentrations of EBT dye (mg/L). Distilled water was used to blank as control before each set of the experiments as control. The adsorption capacity of the unit mass of the Alg-Ch-NPs at equilibrium q_e (mg/g) was calculated by the following equation:

$$q_e = \frac{(C_0 - C_e)v}{w} \quad (2)$$

where v is the volume of the dye solution (L) and w is the weight of the adsorbent (g) added to the solution.

3. Results and discussions

3.1. Characterization of synthesized nanoparticles

3.1.1. UV spectroscopy

Iron NPs usually show black color, depending on the particle size and intensity of the synthesized NPs. When iron solution was exposed into plant extract through alginate gel, the color change occurred due to the reduction of the iron salt into the NPs [24]. The UV-vis spectra of iron solutions with cherry leaf extract, Ca alginate gel and alginate crosslinked cherry NPs are shown in the Fig. 3. The salts reduction of iron solutions by aqueous cherry leaf extract was visualized by changing the color from dark green to black, which indicated the formation of the iron NPs [24]. The spectra of the iron solutions with cherry leaf extract showed the peaks, whereas the alginate crosslinked cherry NPs show no peaks. This phenomenon may be an indication of the formation of cherry leaf extract mediated alginate crosslinked iron NPs.

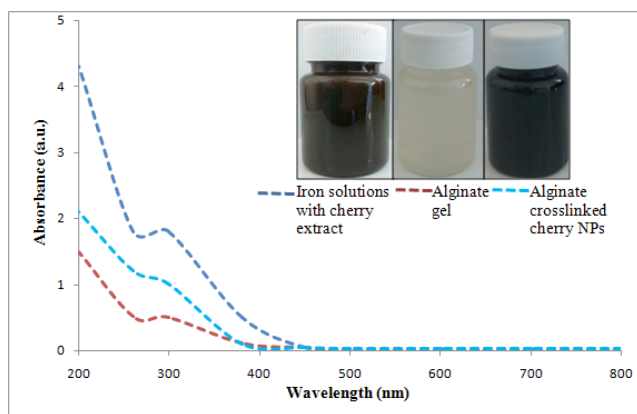


Fig. 3. UV spectra to trace the synthesis of alginate crosslinked cherry NPs.

3.1.2. FTIR analysis

FTIR analysis was employed to analyze possible biomolecules in the spectral range 500–4000 cm^{-1} . The FTIR spectra of iron solution with cherry leaf extract, Ca alginate gel and alginate crosslinked NPs are shown in Fig. 4. The FTIR spectra for cherry leaf extract with iron solution (Fig. 4a), Ca alginate gel (Fig. 4b) and Alginated crosslinked NPs (Fig. 4c) cherry NPs showed different bands (cm^{-1}) which represented the functional groups stretching O-H, C-H, O=C=O, C=C, C-O [25]. FTIR bands for alginate crosslinked NPs at 3463 cm^{-1} could be assigned to O-H vibrations which were evident for the presence of phenol group. Additionally the band around 2927 cm^{-1} might be related to aliphatic C-H vibrations. And the peaks located at 1647 cm^{-1} might be related to the C=C stretching of unsaturated aliphatic structure. Peaks around 1041 cm^{-1} stretching might represent the presence of the alcoholic groups [25].

3.1.3. XRD measurements

The X-Ray diffraction pattern of the synthesized cherry mediated iron NPs and the NPs after encapsulation by alginate are shown in Fig. 5. The formation of alginate encapsulate nanoparticles was confirmed by XRD analysis and the result was confirmed by XRD analyzer. Fig. 5a shows the cherry leaf mediated iron NPs, where the formation mineral phase of maghemite or magnetite was indicated. Due to both of maghemite and magnetite had similar XRD pattern, it is difficult to exclude the formation of maghemite instead of magnetite in the samples. In addition, the XRD pattern of alginate crosslinked green NPs is shown in Fig. 5, indicating that the peaks at 32° is increased. The changes of the NPs peaks confirmed the synthesis of the biomolecule loaded alginate crosslinked NPs [13].

3.1.4. SEM, EDX and TEM analysis

Scanning electron micrographs (SEM) of cherry leaf mediated NPs and the alginate crosslinked NPs are given in Figs. 6a and 6b respectively. In the enlarged view of the SEM micrographs, it was seen that the alginate crosslinked NPs showed more porous structure with larger surface area

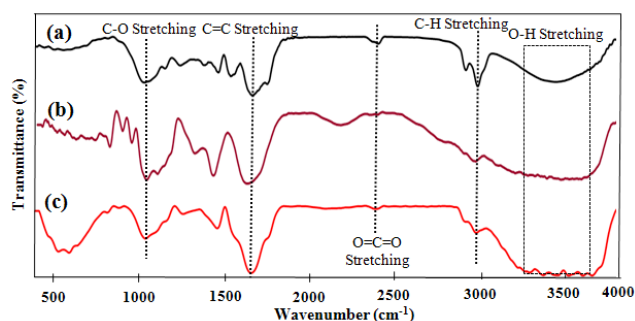


Fig. 4. FTIR spectrum of cherry leaf extract (a) with iron solution (b) Ca alginate gel and (c) Alginated crosslinked NPs.

compared with the cherry leaf extract NPs. Figs. 7a and 7b show the EDX spectra of the cherry leaf NPs and alginate cross linked NPs. The EDX spectra of alginate crosslinked NPs showed the peak of Ca which meant the Ca alginate was successfully capped with the green cherry NPs [26]. Transmission electron microscopy (TEM) analysis revealed the morphology of synthesized NPs (Fig. 8). TEM micrograph of cherry mediated iron NPs was spherical and had smooth surface with the size of the particles from 50.13 to 81.12 nm (Fig. 8a). Whereas the TEM image of alginate crosslinked cherry NPs indicated crystal oval structure with rough surface and the size of the particles was noticed 55.12–80.57 nm (Fig. 8b), which demonstrated that the synthesized Alg-Ch-NPs was nanomaterial [13].

3.2. Point of zero charge (pH_{pzc}) of the adsorbent

Measurement of pH_{pzc} of an adsorbate is very much necessary to know the charge of the surface of adsorbent [24]. pH_{pzc} is measured by drawing two curves, one is $\text{pH}_{\text{initial}}$ versus pH_{final} and the other is $\text{pH}_{\text{initial}} = \text{pH}_{\text{final}}$ (Fig. 9). The intersection point of these two curves indicated the point of zero charge. The zero charge point of Alg-Ch-NPs was identified as 3.40. It meant that the Alg-Ch-NPs acted as positively charged NPs below the pH 3.40, reversely acted as negatively charged surface at the pH above 3.40.

3.3. Effect of pH on dye removal

Adsorption capacity of nanoparticle is solely intimate with the initial pH of adsorbate. The effect of the pH of dye solution on the removal of EBT dyes was studied by varying pH from 2 to 14 under constant parameters (30°C temperature, 150 rpm shaking). The results of the pH study were shown in Fig. 10. The adsorption for EBT dye by Alg-Ch-NPs was became lower at higher pH. At pH 2, the removal percentage (94%) was higher than that at the other pH conditions. The removal percentage of EBT was decreased to 40% at maximum pH. This phenomenon was expected and could be explained by considering pH_{pzc} of the adsorbate and molecular nature of the EBT dye (represents an anionic dye). The pH_{pzc} of the adsorbent was 3.40, which meant that the adsorbent surface would be positively charged below pH 3.40, thereby the dye anions could be better attracted by the electrostatic attraction. Increasing pH caused the com-

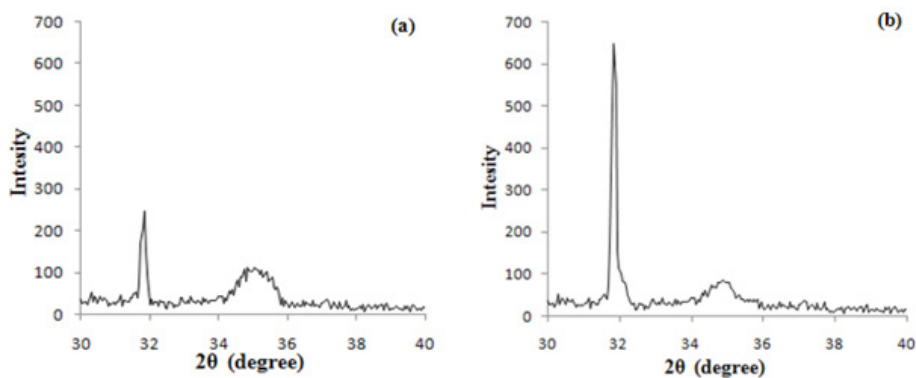


Fig. 5. XRD patterns of cherry leaf mediated iron NPs (a) and Alginate crosslinked NPs (b).

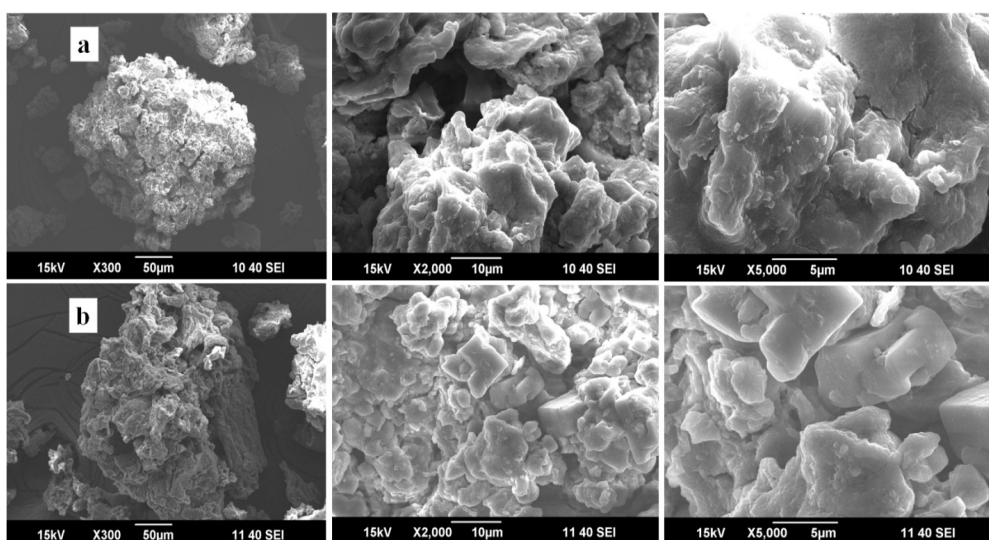


Fig. 6. SEM images of cherry leaf mediated iron NPs (a) and Alginate crosslinked cherry NPs (b).

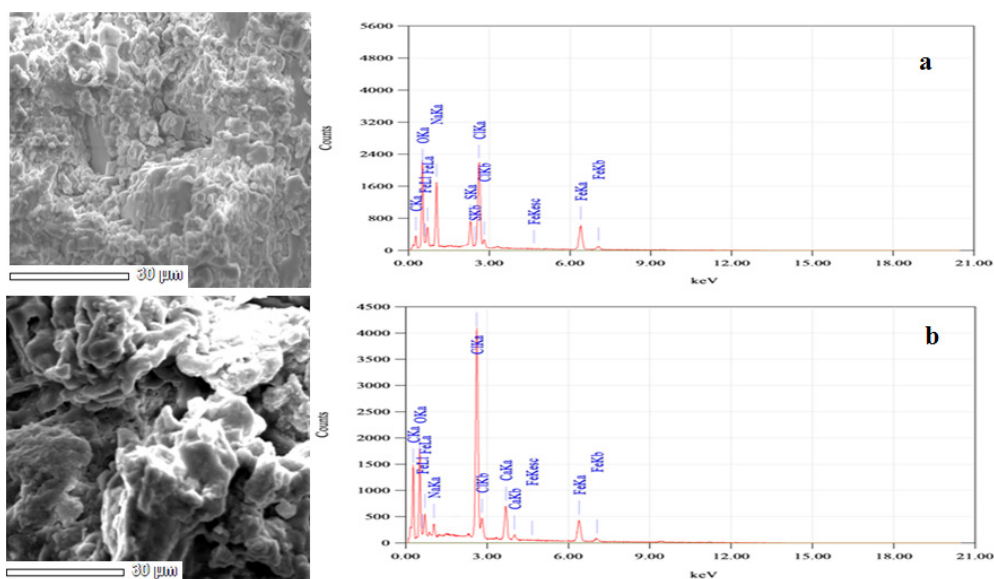


Fig. 7. EDX Spectra of cherry leaf mediated iron NPs (a) and Alginate crosslinked cherry NPs (b).

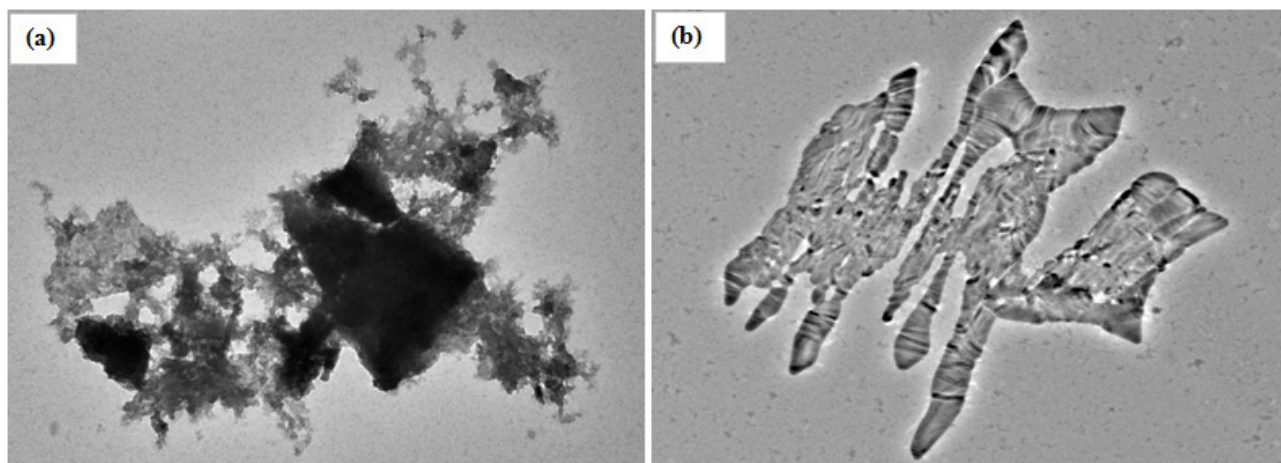


Fig. 8. TEM images of cherry leaves mediated iron NPs (a) and Alginate crosslinked cherry NPs (b).

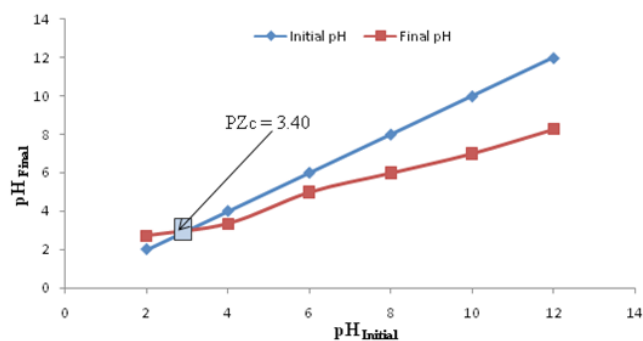


Fig. 9. Determination of zero charge point of Alg-Ch-NPs.

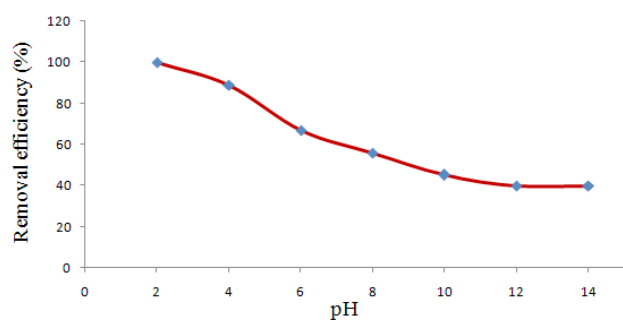


Fig. 10. Effect of pH on the removal of EBT dye by Alg-Ch-NPs.

petition between electrons and dyes anions at adsorption locations [26].

3.4. Effect of initial dye concentration on EBT dye adsorption

The effects of the initial dye concentrations on the EBT dye removal were investigated at different initial concentrations of dye such as 10 mg/L, 50 mg/L, 100 mg/L, 150 mg/L and 200 mg/L, and the other conditions remained unchanged, as shown in Fig. 11. Dye removal percentage of the Alg-Ch-NPs was higher at the beginning of all concentrations due to the availability of higher surface area on

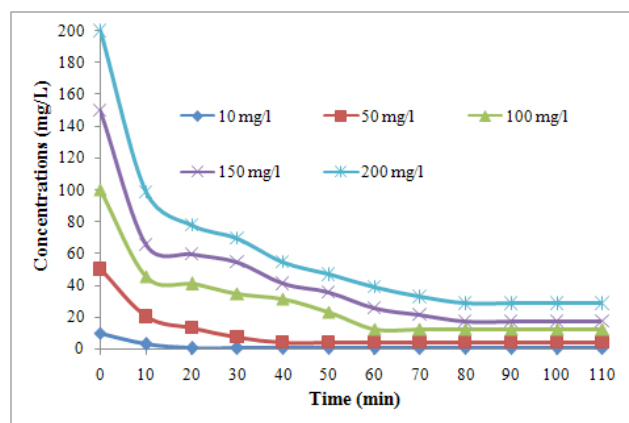


Fig. 11. Effect of initial concentrations of dye on removal of EBT dyes with time.

adsorbent surface [27]. But, the rate of adsorption decreased as time passing until the final or equilibrium concentrations. The removal percentage for different concentrations of dyes was shown to be dependent on time. Higher concentrations of the dye required more time to remove by the Alg-Ch-NPs. From Fig. 11, it was shown that the initial concentrations of dyes had a significant effect on dyes removal trend [5].

In order to find the effect of the initial concentrations of dyes on adsorption capacity of synthesized materials, 0.5 g adsorbent was used in the 100 mL dyes solutions with different concentrations (10–200 mg/L), and the other parameters (30°C temperature, 150 rpm shaking, solution pH 2, adsorbent dose 1 g/L) remained constant. The adsorption capacity of the adsorbents has been plotted in Fig. 12. It showed that the initial concentrations of the dyes had significant effect on the adsorption capacity per unit weight. It also showed that the amount of adsorption (mg/g) increased, as the initial concentration of the dye increased. This phenomenon occurred due to availability of the more dyes molecule in the solution. The maximum adsorption capacity of the prepared Alg-Ch-NPs in this study was 85.66 mg/L, which was satisfactory compared with other

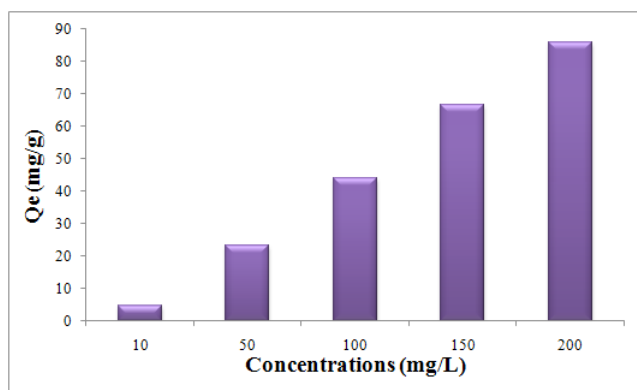


Fig. 12. Effect of the initial concentrations of EBT dye on adsorption capacity of Alg-Ch-NPs.

studies on the removal of EBT dye [28]. Previous studies reported the adsorption capacity of different synthesized materials for EBT dyes shown in Table 2, such as activated carbon prepared from Rice hulls (160.36 mg/g) [29], Bottom ash (94.96 mg/g) [30], Magnetite/silica/pectin nanoparticles (65.35 mg/g) [28], NiFe_2O_4 magnetic nanoparticles (47.0 mg/g) [31], Microwave radiation-treated almond shell (29.41 mg/g) [32], β -Cyclodextrins/polyurethane foam material (20.17) [33], Cold plasma-treated almond shell (18.18 mg/g) [32], Hydrophobic cross-linked polyzwitter ionic acid (HCPZA) (15.9 mg/g) [34], Untreated almond shell (6.02 mg/g) [35].

3.5. Effect of the adsorbent dosages

The experiment on the effect of the Alg-Ch-NPs adsorbent dosages on the EBT dye removal was performed in the range of the dosages 0.1 g/L to 1.2 g/L, and the other parameters (dyes concentrations 100 mg/L, 30°C temperature, 150 rpm shaking, solution pH 2) remained constant. The specific dosages of the NPs were added to the 100 mg/L concentrations dyes solution under the 150 rpm stirring at 30°C temperature. Fig. 13 showed the removal of dyes was increased rapidly upto the dosage 1.5 g/L and then the removal of dye suddenly stopped due to the saturation of adsorbent compared to the presence of dye molecule. The adsorption was faster with the higher dosage due to the surface area of the adsorbent increased the accessibility of the more adsorption sites [35,36].

3.6. Effect of the ionic strength on EBT dye removal using Alg-Ch-NPs

Dyes are usually contains different salts and metal ions. The presence of salts existing in dyes may lead to the effect of ionic strength on the adsorption of dye. Fig. 14 showed the effect of the ionic strength on EBT dye removal from aqueous solution by Alg-Ch-NPs. It was found that the presence of NaCl in the adsorption solution increased the removal percentage of EBT dye when the other parameters (dyes concentrations 100 mg/l, 30°C temperature, 150 rpm shaking, solution pH 2, adsorbent dose 1 g/L) was constant. The result showed that the adsorption of dye

Table 2

Adsorption capacities of different materials for adsorption of EBT dye

Adsorbent	Adsorption capacity (mg/g)	References
Activated carbon prepared from rice hulls	160.36	[29]
Bottom ash	94.96	[30]
Magnetite/silica/pectin nanoparticles	65.35	[28]
NiFe_2O_4 magnetic nanoparticles	47.0	[31]
Microwave radiation-treated almond shell	29.41	[32]
β -Cyclodextrins/polyurethane foam material	20.17	[33]
Cold plasma-treated almond shell	18.18	[32]
Hydrophobic cross-linked polyzwitter ionic acid (HCPZA)	15.9	[34]
Untreated almond shell	6.02	[35]
Alg-Ch-NPs	85.66	[This study]

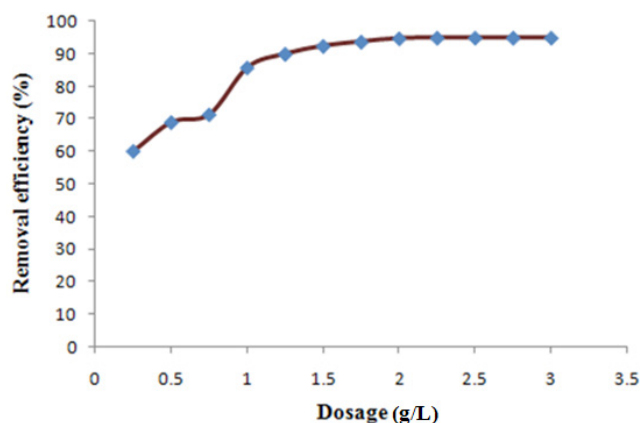


Fig. 13. Effect of different dosages of Alg-Ch-NPs on EBT dye removal.

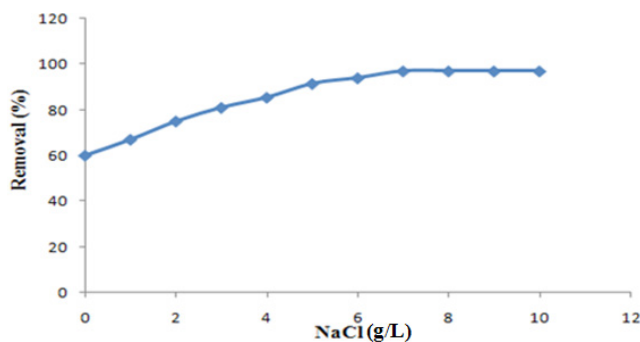


Fig. 14. Effect of salinity on the EBT dye absorption by using Alg-Ch-NPs.

by Alg-Ch-NPs was getting faster by adding NaCl. It might be because the adsorption of the dye was dominated by ion-exchange process [37]. The result can be explained as Alg-Ch-NPs might get more positive charges to adsorb the anionic EBT dye after adding NaCl into the solution. This situation was expected and also previously reported by other studies [38].

3.7. Adsorption mechanism

In the assumed adsorption model (Fig. 15), the anions of the EBT dyes were adsorbed on the surface of the Alg-Ch-NPs because of its positive surface. In Figs. 16a and 16b, the FTIR spectra was showed before and after adsorption, respectively. Fig. 16a showed the peaks at 3440 cm^{-1} , 2947 cm^{-1} , 2374 cm^{-1} , 1656 cm^{-1} , 1514 cm^{-1} , 1049 cm^{-1} and 609 cm^{-1} , which represented O-H, C-H, O=C=O, C=O, C-O and C-Br stretching respectively [39]. On the other hand, the peaks were shown for the sample after adsorption (Fig. 16b) at 3494 cm^{-1} , 2945 cm^{-1} , 2374 cm^{-1} , 1674 cm^{-1} , 1452 cm^{-1} , 1333 cm^{-1} , 1085 cm^{-1} and 659 cm^{-1} [40]. The new peak at 1330 cm^{-1} is represented the presence of the N-O stretching. The shifting of the peak values after adsorption might be an indication of the chemical interactions between the functional groups in Alg-Ch-NPs and EBT dyes [5]. The broadening of the hydroxyl (–OH) group peaks at 3440 cm^{-1} indicated that hydroxyl group on EBT dye was bio-adsorbed onto Alg-Ch-NPs [39].

3.8. Adsorption isotherm studies

Adsorption isotherms are important to describe the phenomena in the adsorption study, which mainly retain substance from the liquid to a solid phase [20]. As well as the adsorption isotherm describes the interactions between adsorbent and adsorbate [25]. There are different equations such as Langmuir, Freundlich, Dubinin-Radushkevich, Redlich Peterson, Flory Huggins, Temkin and Sips etc. to describe the experimental isotherms and developed iso-

therm model. Here, Langmuir, Freundlich and Temkin models were used in isotherm studies in this study [40].

Langmuir isotherm model usually describe the gas solid phase adsorption, assuming that monolayer adsorption occurs at definite local sites. This model supports homogenous adsorption including molecules with homogenous enthalpies and sorption activation energy. Langmuir isotherm model can be characterized by plateau and equilibrium saturation point and can be expressed as follows [23]:

$$q_e = \frac{q_{\max} k_{LC} c_e}{1 + k_{LC} c_e} \quad (3)$$

where c_e is the concentration of dye at equilibrium stage and k_L represents Langmuir constant. q_{\max} is the monolayer

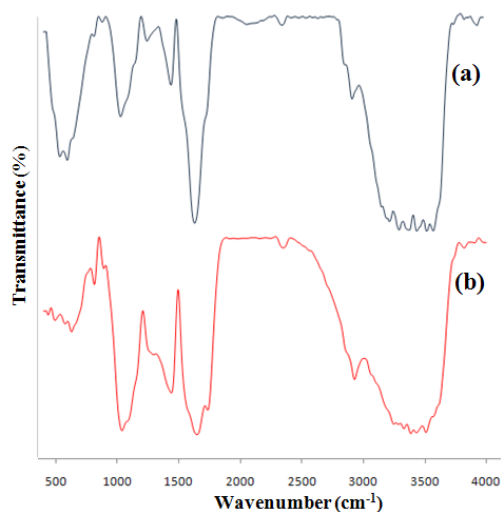


Fig. 16. FTIR spectra of Alg-Ch-NPs (a) before adsorption and (b) after adsorption.

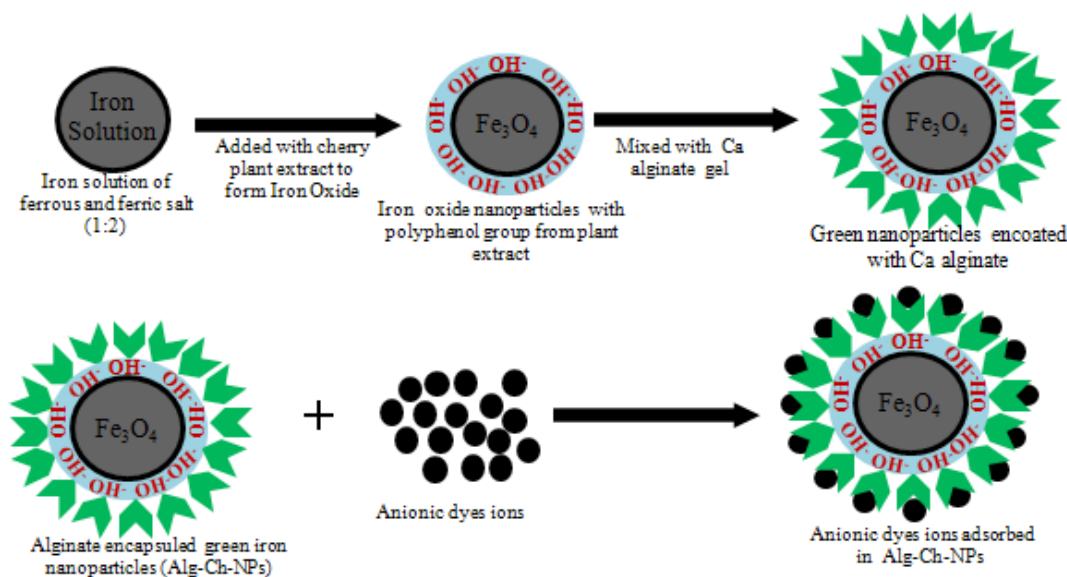


Fig. 15. Proposed adsorption mechanisms of EBT dye using Alg-Ch-NPs.

capacity of the synthesized NPs. The constant k_L and q_{max} can be measured from the intercept and slope of the linear plot of c_e and c_e/q_e shown in Fig. 17a.

Freundlich isotherm model generally describes the reversible and non-ideal adsorption. This model supports the multi layer adsorption over heterogeneous surface of the adsorbent [14]. The surface heterogeneity or the adsorption intensity shown by the range of slope between 0 and 1, i.e. the value close to zero means the surface is more heterogeneous. If the value of the adsorption intensity ($1/n$) is less than 1, it indicates the chemisorptions process, while the value of adsorption intensity is more than 1, it indicates the cooperative process. Freundlich isotherm model was described by the following equation:

$$q_e = k_F c_e^{1/n} \tag{4}$$

where K_F notify the adsorption capacity. The isotherm type can be assumed with the value of $1/n$. If the value lies $0 < 1/n < 1$, the isotherm is favorable. If the value is equal to 0, it indicates the irreversible isotherm and the value is more than 1, it means unfavorable isotherm. The value of n and K_F has been taken from slope and intercept of the plot $\ln q_e$ vs $\ln c_e$ shown in Fig. 17b.

Tempkin isotherm model is very much useful for denoting the gas phase equilibrium. Interaction between adsorbates and adsorbents is the matter of considerations for this model [14]. As well as, the assumption of this model is that the binding energy is uniformly distributed. The equation describes the tempkin model as follows:

$$q_e = RT/b \ln k_T c_e \tag{5}$$

where b is the Tempkin isotherm constant and k_T is the equilibrium binding constant. The values of the constants were taken from the slope and intersect of $\ln q_e$ vs $\ln c_e$ shown in Fig. 17c.

The parameters of the Langmuir, Freundlich and Tempkin isotherm models were obtained by the linear plots of c_e/q_e vs c_e , $\ln q_e$ vs $\ln c_e$ and q_e vs $\ln c_e$ respectively and are summarized in Table 3. Comparing the value of R^2 for all isotherm models, it was found that the R^2 value for Freundlich isotherm model was highest. Thus, from the above discussions and comparisons of different model data, it can be concluded that this work is very consistent with the Freundlich isotherm model. The adsorption in this study was the multi layer adsorption over heterogeneous surface of the adsorbent. In addition, reversible and non-ideal adsorption occurred and the value of n in Table 3 indicated that the type of adsorption was chemisorption.

Table 3
Parameters of isotherms and kinetics models on adsorption of EBT dye using Alg-Ch-NPs

Name of the models	Parameters		
Langmuir isotherm	k_L (L mg ⁻¹)		R^2
	0.86		0.881
Freundlich isotherm	k_F (mg/g)	n	R^2
	1.312	1.18	0.993
Tempkin isotherm	b (kJ mol ⁻¹)	k_T (L g ⁻¹)	R^2
	86.7	0.469	0.875
Pseudo first order	k_1 (min ⁻¹)		R^2
	4.1×10^{-2}		0.966
Pseudo second order	k_2 (g/mg min)		R^2
	0.31×10^{-2}		0.957
Intraparticle diffusion	k_{id} (mg/g ^{1/2})	C	R^2
	12.82	11.19	0.966

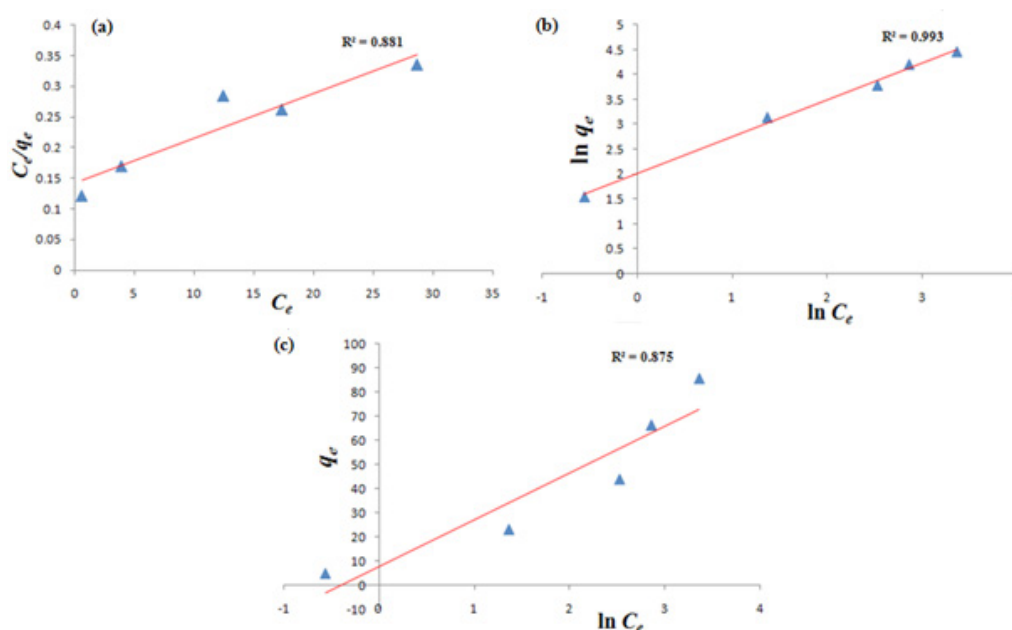


Fig. 17. Plots of (a) Langmuir isotherm (c_e vs c_e/q_e) (b) Freundlich isotherm model ($\ln c_e$ vs $\ln q_e$) (c) Tempkin isotherm model ($\ln c_e$ vs q_e).

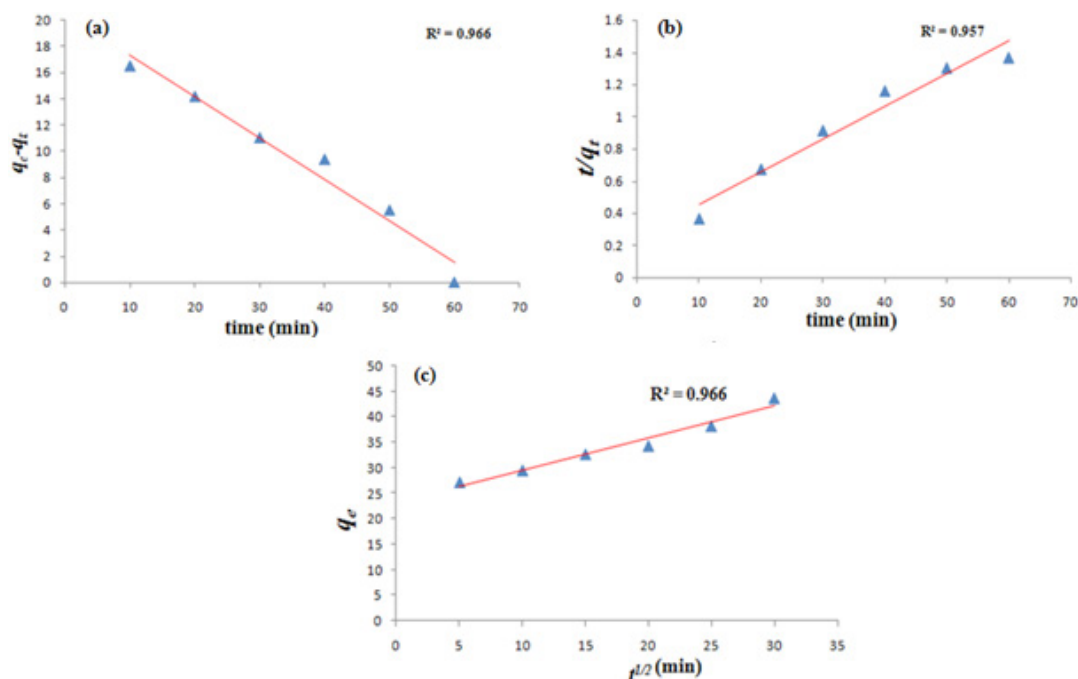


Fig. 18. Plots of (a) Pseudo first order kinetics model (t Vs $q_e - q_t$) (b) Pseudo second order kinetics model (t Vs t/q_t) and (c) Intraparticle diffusion model ($t^{1/2}$ Vs q_e).

3.9. Studies on adsorption kinetic

Removal of dyes by using synthesized Alg-Ch-NPs depends on the interaction between dye and the surface of the adsorbent particles. The dye removal synthesized sample was evaluated in terms of dye removal kinetics by measuring the dye at different times. Pseudo-first order and second order models were used for characterizing the kinetics data for removal of dye ion [40]. The linearized pseudo first order equation was expressed as follows:

$$\log(q_e - q_t) = \log q_e - \frac{t}{2.303} k_1 \quad (6)$$

where q_t is the amount of dye adsorbed at time t and q_e is the amount of adsorbing dye at equilibrium stage. k_1 is the pseudo-first-order rate constant measured from the plot t versus $q_e - q_t$ (Fig. 18a).

Pseudo-second-order equation is expressed as follows:

$$\frac{t}{q_t} = \frac{1}{K^2 q_e^2} + \frac{1}{q_e} t \quad (7)$$

where the q_e is the equilibrium adsorption capacity, and the second order constant k_2 can be determined experimentally from the slope and intercept of the plot t/q_t versus t (Fig. 18b).

The pseudo-first-order rate and the pseudo-second-order rate constants with their value of R^2 are presented in Table 3. R^2 is one of the most important determinants to determine the best fitting model for experimental data [41]. From the Table 3 it is clear that the R^2 (0.966) for pseudo-first-order is higher than that of R^2 (0.957) for pseudo-second-order. Therefore, on the basis of the value of R^2 , it can be concluded that pseudo-second-order model is most suitable for the experimental data.

Weber's intraparticle diffusion model was also fitted to gain the adsorption mechanisms and the adsorption rate [40]. To elucidate the diffusion mechanism the kinetic results were analyzed with the following expression:

$$q_t = k_{id} t^{1/2} + C \quad (8)$$

where C is the intercept and k_{id} intraparticle diffusion rate constant ($\text{mg/g h}^{1/2}$), which can be evaluated from the slope of q_t Vs $t^{1/2}$ (Fig. 18c). The calculated value of k_{id} , C and R^2 are shown in Table 3. The intercept of the plot reflects the boundary layer effect [41].

4. Conclusions

The use of synthesized alginate crosslinked green NPs to remove the EBT dye from aqueous solutions was studied in batch experiments. The significant feature of the Alg-Ch-NPs is that EBT dye adsorption capacity is higher compared with previous EBT adsorption studies. The data accorded with the Freundlich isotherm model which concludes the multi layer adsorption over heterogeneous surface and the type of adsorption was chemisorption. In addition, the kinetics of the experimental data followed pseudo-second-order rate equation. Weber's intraparticle diffusion model was also fitted to gain the adsorption mechanisms and find boundary layer effect of the adsorbents. An overall selectivity of the EBT dye was observed that the synthesized cherry mediated alginate crosslinked nanoparticles could be used effectively to remove anionic dye from aqueous solutions. Finally, it can be concluded that the cherry leaf mediated alginate nanoparticles are efficient, cost effective and environmentally friendly adsorbent for the treatment

of industrial wastewater containing dye. There has enough scope for future researchers to work further on the technology described with more functionalization of the NPs and further application on other pollutants such as heavy metals.

Acknowledgements

This work was supported by the State Key Laboratory of Environmental Criteria and Risk Assessment (SKLECR-RA2013FP12) and the Shandong Province Key Research and Development Program (2016GSF115040). The first author would also like to thanks the Chinese Scholarship Council, China (CSC No: 2016GXYO18) for the financial support.

References

- [1] R. Prabhakar, S.R. Samadder, Jyotsana, Aquatic and terrestrial weed mediated synthesis of iron nanoparticles for possible application in wastewater remediation, *J. Clean. Prod.*, 168 (2017) 1201–1210.
- [2] K.S. Siddiqi, A.U. Rahman, Tajuddin, A. Husen, Biogenic fabrication of iron/iron oxide nanoparticles and their application, *Nano. Res. Lett.*, 11 (2016) 498.
- [3] I. Ali, New generation adsorbents for water treatment, *Chem. Rev.*, 112 (2012) 5073–5091.
- [4] G. Asgari, B. Roshani, G. Ghanizadeh, The investigation of kinetic and isotherm of fluoride adsorption onto functionalize pumice stone, *J. Haz. Mat.*, 17 (2012) 123–132.
- [5] I. Ali, C. Peng, I. Naz, Z.M. Khan, M. Sultan, T. Islam, I.A. Abbasi, Phytogenic magnetic nanoparticles for wastewater treatment: a review, *RSC Adv.*, 7 (2017) 40158–40178.
- [6] T. Islam, C. Peng, I. Ali, I.A. Abbasi, Comparative study on anionic and cationic dyes removal from aqueous solution using different plant mediated magnetic nano particles, *Ind. J. G. M. Sci.*, 47 (2018) 598–603.
- [7] T. Phenrat, N. Saleh, K. Sirk, R.D. Tilton, G.V. Lowry, Aggregation and sedimentation of aqueous nanoscale zerovalent iron dispersions, *Env. Sci. Tech.*, 41 (2006) 284–290.
- [8] S. Srivastava, S.B. Agrawal, M.K. Mondal, Biosorption isotherms and kinetics on removal of Cr(VI) using native and chemically modified *Lagerstroemia speciosa* bark, *Ecol. Eng.*, 85 (2015) 56–66.
- [9] L. Zeng, T. Zhu, Y. Gao, Y. Wang, C. Ning, L. Olofjorn, D. Chen, S. Li, Effects of Ca addition on the uptake, translocation, and distribution of Cd in *Arabidopsis thaliana*, *Ecotoxic. Env. Safety*, 139 (2017) 228–237.
- [10] R. Rajan, K. Chandran, S.L. Harper, S.I. Yun, P.T. Kalaichelvan, Plant extract synthesized silver nanoparticles: an ongoing source of novel biocompatible materials, *Ind. Crops Prod.*, 70 (2015) 356–373.
- [11] L. Carro, E. Hablot, T. Coradin, Hybrids and biohybrids as green materials for a blue planet, *J. Sol–Gel Sci. Tech.*, 70 (2014) 263–271.
- [12] K.H. Chu, M.A. Hashim, Copper biosorption on immobilized seaweed biomass: column breakthrough characteristics, *J. Env. Sci. China*, 19 (2007) 928–932.
- [13] A.A. Sujima, A. Sahi, P. Venkatachalam, Synthesis of bioactive chemicals cross-linked sodium tripolyphosphate (TPP) – Chitosan Nanoparticles for enhanced cytotoxic activity against human ovarian cancer cell line (PA-1), *J. Nanomed. Nanotech.*, 76 (2016).
- [14] A. Beduoi, M.F. Ahmadi, N. Bensalah, A. Gadri, Comparative study of Eriochrome black T treatment by BDD-anodic oxidation and Fenton process, *Chem. Eng. J.*, 146 (2009) 98.
- [15] M.A.K.M. Hanafiah, W.S. Wannang, S.H. Zolkafly, L.C. Teong, Z.A.A. Majid, Acid blue 25 on base treated *Shoreadasyphylla* sawdust: kinetic isotherm, thermodynamic and spectroscopic analysis, *J. Env. Sci.*, 24 (2012) 261.
- [16] A.N. Ejhieh, M. Khorsandi, Photodecolorization of Eriochrome Black T using NiSP zeolite as a heterogeneous catalyst, *J. Haz. Mat.*, 176 (2010) 629.
- [17] N. Mohammadi, H. Khani, V.K. Gupta, E. Amereh, S. Agarwal, Adsorption process of methyl orange dye onto mesoporous carbon material—kinetic and thermodynamic studies, *J. Coll. Inter. Sci.*, 362 (2011) 457.
- [18] A.A. Ahmad, B.H. Hameed, Fixed-bed adsorption of reactive azo dye onto granular activated carbon prepared from waste, *J. Haz. Mat.*, 175 (2009) 298.
- [19] O. Gercel, H.F. Gercel, A.S. Kopal, U.B. Ogutveren, Removal of disperse dye from aqueous solution by novel adsorbent prepared from biomass plant material, *J. Haz. Mat.*, 160 (2008) 668.
- [20] N. Mariam, J.N. Lukmanulhakin, M. Shamsuddin, Catalytic reduction of methyl blue using biosynthesised gold nanoparticles, *Malay. J. Cat.*, 2 (2016) 57–61.
- [21] A. Khalid, M. Zubair, Ihsanullah, A comparative study on the adsorption of eriochrome black T dye from aqueous solution on graphene and acid modified graphene, *Arab. J. Sci. Eng.*, 17 (2017) 2543.
- [22] L.P. Lingamdinne, Y. Chang, J. Yang, P. Attri, Biogenic reductive preparation of magnetic inverse spinel iron oxide nanoparticles for the adsorption removal of heavy metals, *The Chem. Eng. J.*, 307 (2017) 74–84.
- [23] I. Langmuir, The adsorption of gases on plane surfaces of glass, mica and platinum, *J. American Chem. Society*, 40 (1918) 1361–1403.
- [24] C. Prasad, S. Karlapudi, C.N. Rao, P. Venkateswarlu, I. Bahadur, A highly resourceful magnetically separable magnetic nanoparticles from aqueous peel extract of *Bottle gourds* for organic dyes degradation, *J. Magn. Mater.*, 243 (2017) 611–615.
- [25] B. Fouconnier, J.E. Terrazas-Rodriguez, F. Lopez-Serrano, Monitoring styrene Pickering SiO₂-supported emulsion polymerization kinetics by Raman spectroscopy: Elucidating mechanisms interpreting the silanol/phenyl π -interactions, *J. Macromol. Sci.*, 54 (2017) 509–515.
- [26] S. Shalini, L. Dorstyn, S. Dawar, S. Kumar, Old, new and emerging functions of casepases, *Cell Death Diff.*, 22 (2015) 526–539.
- [27] A.F. Hassan, A.M. Abdel-Mohsen, M.G.M. Fouda, Comparative study of calcium alginate, activated carbon, an their composite beads on methyl blue adsorption, *Car. Poly.*, 102 (2014) 192–198.
- [28] O.A. Attallah, M.A. Al-Ghobashy, M. Nebsen, M.Y. Salem, Removal of cationic and anionic dyes from aqueous solution with magnetite/pectin and magnetite/silica/pectin hybrid nanocomposites: kinetic, isotherm and mechanism analysis, *RSC Adv.*, 6 (2016) 11461–11480.
- [29] M.D.G.D. Luna, E.D. Flores, C.M. Genuino, F. Futral, M.W. Wan, Adsorption of Eriochrome Black T (EBT) dye using activated carbon prepared from waste rice hulls—optimization, isotherm and kinetic studies, *J. Tai. Inst. Chem. Eng.*, 44 (2013) 646–653.
- [30] A. Mittal, V.K. Gupta, Adsorptive removal and recovery of the azo dye Eriochrome Black T, *Toxic. Environ. Chem.*, 92 (2010) 1813–1823.
- [31] F. Moeinpour, A. Alimoradi, Kazemi, Efficient removal of Eriochrome Black-T from aqueous solution using NiFe₂O₄ magnetic nanoparticles, *J. Environ. Health Sci. Eng.*, 12 (2014) 112.
- [32] O. Sahin, C. Saka, S. Kutluay, Cold plasma and microwave radiation applications on almond shell surface and its effects on the adsorption of Eriochrome Black T, *J. Ind. Eng. Chem.*, 19 (2013) 1617–1623.
- [33] K. Dong, F. Qiu, X.X.U. Guo, J. Yang, D. He, Adsorption behavior of azo dye Eriochrome Black T from aqueous solution by β -cyclodextrins/polyurethane foam material, *Poly. Plast. Tech. Eng.*, 52 (2013) 452–460.
- [34] T.A. Saleh, A.M. Muhammad, S.A. Ali, Synthesis of hydrophobic cross-linked polyzwitter ionic acid for simultaneous sorption of Eriochrome Black T and chromium ions from binary hazardous waters, *J. Coll. Interface Sci.*, 468 (2016) 324–333.

- [35] D. Kavitha, C. Namasivayam, Experimental and kinetic studies on methylene blue adsorption by coir pith carbon, *Biores. Tech.*, 98 (2007), 14–21.
- [36] O. Hamdaoui, Batch study of liquid-phase adsorption of methylene blue using cedar sawdust and crushed brick, *J. Haz. Mat.*, 135 (2006) 264–273.
- [37] D. Ghosh, K.G. Bhattacharyya, Adsorption of methylene blue on kaolinite, *Appl. Clay Sci.*, 20 (2002) 295–300.
- [38] G.O. El-Sayed, Removal of methylene blue and crystal violet from aqueous solutions by palm kernel fiber, *Desalination*, 272 (2011) 225–232.
- [39] P. Geetha, M.S. Latha, M. Koshy, Biosorption of malachite green dye from aqueous solution by calcium alginate nanoparticles: Equilibrium study, *J. Mol. Liq.*, 212 (2015) 723–730.
- [40] M. Martinez-Cabanas, M. Lopez-Garcia, J.L. Barriada, R. Herrero, M.E.S.D. Vicente, Synthesis and application of surfactants coated magnetite nanoparticles for demulsification of crude oil in water emulsion, *Chem. Eng. J.*, 301 (2016) 83–91.
- [41] H.L. Chieng, L.B.L. Lim, N. Priyantha, Sorption characteristics of peat from Brunei Darussalam for the removal of rhodamine B dye from aqueous solution: adsorption isotherms, thermodynamics, kinetics and regeneration studies, *Desal. Water Treat.*, 55 (2015) 664–677.